

Blood-flow magnetic resonance imaging of the retina

Yingxia Li,^{a,1} Haiying Cheng,^{a,1} and Timothy Q. Duong^{a,b,c,*}

^aYerkes Imaging Center, Emory University, Atlanta, Georgia, USA

^bDepartments of Neurology and Radiology, Emory University, Atlanta, Georgia, USA

^cAtlanta Veterans Affairs Medical Center, Decatur, Georgia, USA

Received 23 August 2007; revised 28 September 2007; accepted 24 October 2007
Available online 1 November 2007

This study describes a novel MRI application to image basal blood flow, physiologically induced blood-flow changes, and the effects of isoflurane concentration on blood flow in the retina. Continuous arterial-spin-labeling technique with a separate neck coil for spin labeling was used to image blood flow of the rat retina at $90 \times 90 \times 1500$ - μm resolution. The average blood flow of the whole retina was 6.3 ± 1.0 ml/g/min under 1% isoflurane, consistent with the high blood flow in the retina reported using other techniques. Blood flow is relatively constant along the length of the retina, except it dipped slightly around the optic nerve head and dropped significantly at the distal edges where the retina terminates. Hyperoxia (100% O₂) decreased blood flow $25 \pm 6\%$ relative to baseline (air) due to vasoconstriction. Hypercapnia (5% CO₂ + 21% O₂) increased blood flow $16 \pm 6\%$ due to vasodilation. Increasing isoflurane (a potent vasodilator) concentration to 1.5% increased blood flow to 9.3 ± 2.7 ml/g/min. Blood-flow signals were confirmed to be genuine by repeating measurements after the animals were sacrificed in the MRI scanner. This study demonstrates a proof of concept that quantitative blood flow of the retina can be measured using MRI without depth limitation. Blood-flow MRI has the potential to provide unique insights into retinal physiology, serve as an early biomarker for some retinal diseases, and could complement optically based imaging techniques.

© 2007 Elsevier Inc. All rights reserved.

Keywords: High-resolution MRI; Perfusion; Arterial spin labeling (ASL); Choroidal and retinal vessels; BOLD; Hypercapnia; Hyperoxia; CBF; Isoflurane

Introduction

Blood flow in the retina is tightly regulated and intricately coupled to basal metabolic function under normal physiological conditions (Riva et al., 2005). Perturbations of basal blood flow and its coupling to metabolic function have been implicated in many retinal diseases, such as retinal ischemia and diabetic retinopathy, which could lead to acute or gradual loss of vision. The retina is a part of the central nervous system and it is nourished by two different vascular supplies, namely, the *retinal* and *choroidal* circulations (Harris et al., 1998). *Retinal* vessels are found on the surface of the retina and embedded in the ganglion cell layer and the inner nuclear layer. *Choroidal* vessels are located behind the outer nuclear layer, underneath the retinal pigmented epithelium.

Blood flow in the retina has been studied using microsphere techniques (Wang et al., 2007), fluorescein angiography (Preussner et al., 1983), indocyanin-green angiography (Guyer et al., 1993), laser Doppler flowmetry (LDF) (Formaz et al., 1997), and laser speckle imaging (Cheng and Duong, 2007) (reviewed in Riva et al., 2005). These techniques have made remarkable contributions to our understanding of normal retinal physiology and pathophysiology. Microsphere techniques require the animals to be sacrificed but provide quantitative blood-flow values, whereas the other techniques mentioned above are optically based and non-invasive but measure only qualitative blood flow, predominantly in large surface vessels which may not accurately reflect local tissue perfusion. Measuring blood flow in the *choroidal* vessels using optical techniques is difficult because the *choroidal* vessels are hidden from view by the retinal pigment epithelium. Optically based imaging techniques also have limited field of view constrained by illumination angle. Moreover, optical scattering and disease-induced opacity of the vitreous humor, cornea and lens, such as vitreal hemorrhage and cataract, could hamper efficacy of optically based retinal imaging techniques.

Magnetic resonance imaging (MRI), in contrast, is a non-invasive imaging method that provides *in vivo* structural, physiological (i.e., blood flow and oxygenation), and functional information without depth limitation. Blood flow can be imaged by

Abbreviations: ASL, arterial spin labeling; LDF, laser Doppler flowmetry; BOLD, blood-oxygen-level-dependent; PVE, partial-volume effect.

* Corresponding author. Yerkes Imaging Center, Emory University, Atlanta, Georgia, USA.

E-mail address: tduong@emory.edu (T.Q. Duong).

¹ Li and Cheng contributed equally to this work.

Available online on ScienceDirect (www.sciencedirect.com).

using an exogenous intravascular contrast agent or by magnetically labeling the endogenous water in blood (Calamante et al., 2002 for review). The latter, commonly referred to as the arterial spin-labeling (ASL) technique, is widely utilized to measure quantitative basal blood flow and dynamic blood-flow changes associated with functional stimulations in the brain (Calamante et al., 2002). ASL MRI is more sensitive to blood flow in small vessels and provides a measure of tissue perfusion, as opposed to large vessels. The main drawback of MRI is that it has lower spatial resolution compared to optical imaging techniques.

Advances in MRI technologies over the past decade have significantly improved spatial resolution and sensitivity. MRI has recently been applied to investigate structures of the retina (Berkowitz et al., 2006; Cheng et al., 2006; Shen et al., 2006), as well as changes in tissue oxygenation using blood-oxygen-level-dependent (BOLD) functional MRI associated with physiologic (Cheng et al., 2006) and visual (Duong et al., 2002) stimulation in the retina. Changes in layer thickness and BOLD functional MRI responses to physiologic challenges in an animal model of retinitis pigmentosa in which the photoreceptors progressively degenerate have also been reported (Cheng et al., 2006). These studies together demonstrated that high-resolution MRI of the retina is feasible. Signal-to-noise ratio of blood-flow MRI is, however, two orders of magnitude lower than that of the typical anatomical and functional MRI in part because the blood volume in the central nervous system is only 3–5% of total tissue volume. While basal blood flow, stimulus-evoked, and pathology-induced blood-flow changes have been well described in the brain (Calamante et al., 2002), blood-flow MRI application in the retina has not yet been demonstrated because very high spatial resolution is needed to visualize the thin retina of only 267 μm thick, including the choroid (Cheng et al., 2006).

This study explored the feasibility of imaging blood flow in the rat retina using MRI at $90 \times 90 \times 1500\text{-}\mu\text{m}$ resolution without depth limitation. Blood-flow measurements were made using the highly sensitive continuous ASL technique with a separate neck coil for spin labeling and the snap-shot echo-planar-imaging acquisition. Quantitative basal blood flow, physiologically induced blood-flow changes, and the effects of isoflurane concentration on blood flow were investigated in the normal retinas.

Materials and methods

Animal preparation

Experiments were performed on normal adult male Sprague–Dawley rats (350–400 g, $N=6$) anesthetized with 1% isoflurane, paralyzed with pancuronium bromide (3 mg/kg first dose, 1 mg/kg/h, ip), and mechanically ventilated. Measurements were also made using 1.5% isoflurane on another group of animals ($N=4$). End-tidal CO_2 (Surgivet capnometer, Waukesha, WI), heart rate and arterial oxygen saturation (Nonin-8600, Plymouth, MN), and rectal temperature (Digisense, Cole Palmer, Vernon Hills, IL) were continuously monitored and maintained within normal physiological ranges. Non-invasive end-tidal CO_2 values were previously calibrated against invasive blood-gas samplings under identical setting. To avoid being invasive on all animals, femoral arteries were catheterized only in some animals for blood-gas sampling for routine assessment. All sampled blood gases and physiological

parameters were within normal physiological ranges unless purposefully altered.

Inhalation stimuli

Hyperoxic (100% O_2) and hypercapnic (5% CO_2 , 21% O_2 , balance N_2) challenges were used to modulate blood flow. Ambient air was used as baseline. Images were acquired continuously for 6 min during baseline and 6 min during hyperoxic or hypercapnic challenge. A break of 10–15 min intervals was given between trials. Typically, 2–3 trials of both hyperoxia and hypercapnia were studied on the same animal and the presentation order of different physiologic challenges was random, with the entire study lasting ~ 3 h including animal preparation.

MRI methods

MRI studies were performed on a Bruker 7-Tesla/30-cm magnet and a 40 G/cm B-GA12 gradient insert (Bruker, Billerica, MA). Rats were placed onto a head holder consisting of ear and tooth bars. A small circular surface coil (inner diameter ~ 7 mm) was placed on the left eye. A butterfly neck coil, built into the animal holder, was placed at the neck position for continuous arterial spin labeling (Williams et al., 1992; Shen et al., 2005). The two coils were actively decoupled. Magnetic field homogeneity was optimized using FASTMAP shimming with an isotropic voxel encompassing the entire eye.

Scout anatomical images at three orthogonal axes were acquired to guide placement of a single mid-axial imaging slice bisecting the center of the eye and the optic nerve head. Blood-flow MRI was acquired using the continuous ASL technique (Williams et al., 1992; Shen et al., 2005) with four-segment, gradient-echo echo-planar imaging (EPI). Paired images were acquired in an interleaved fashion—one with arterial spin labeling and the other without spin labeling. Continuous arterial spin labeling employed a 2.9-s square RF pulse to the labeling coil in the presence of 1.0 G/cm gradient along the flow direction. The sign of the frequency offset was switched for non-labeled images. The labeling plane is perpendicular to the flow direction at the neck position. The other MRI parameters were: field of view $\text{FOV}=11.5 \times 11.5$ mm, matrix 128×128 (90×90 μm), slice thickness = 1.5 mm, a repetition time (TR) = 3.0 s per segment (90° flip angle), and echo time (TE) = 14 ms. The total time for each trial was 6 min baseline and 6 min physiologic stimulations.

Data analysis

Image analysis employed codes written in Matlab (MathWorks Inc., Natick, MA) and STIMULATE software (University of Minnesota). All reported values and error bars on graphs were in mean \pm SD. All statistical tests employed Student *t*-test with $P < 0.05$ indicating statistical significance. Basal blood-flow data were derived from the data obtained during baseline of the physiologic stimulations.

Image co-registration

Images were acquired in time series, and corrected for motion and drift before averaging pixel-by-pixel off-line as described previously (Cheng et al., 2006).

Blood-flow calculation

Blood-flow signals (S_{CBF}) with intensity in units of ml/g/min were calculated pixel-by-pixel using $S_{\text{CBF}} = \lambda/T_1 [(S_C - S_L)/(S_L +$

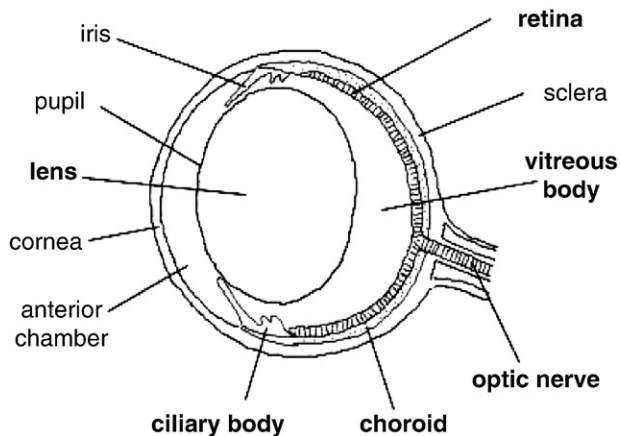


Fig. 1. A cartoon of the rat eye, depicting the retina and choroid complex, vitreous body, ciliary body, lens, and optic nerve.

$(2\alpha - 1)S_C]$ (Shen et al., 2005), where S_C and S_L are signal intensities of the control and labeled images, respectively. λ is the water tissue-blood partition coefficient and was taken to be 0.9 (Herscovitch and Raichle, 1985). Brain T_1 of 1.8 s at 7 T was used (Barbier et al., 2005). α , the arterial spin-labeling efficiency, was measured to be 0.8 (Shen et al., 2005).

Cross-correlation analysis

Percent-change color maps for display purpose were obtained using cross-correlation analysis with >90% confidence level by matching the blood-flow signal time courses to the expected stimulus paradigm. Percent-change color maps were overlaid on blood-flow images. A minimal cluster size of 2 contiguous pixels was further imposed with a resultant $P \ll 0.01$.

Blood-flow analysis

To objectively analyze blood-flow data and minimize partial-volume effect (PVE), automated profile analysis (Cheng et al., 2006) was performed instead of region-of-interest analysis as previously described. Briefly, the retina was first detected using an edge-detection technique. Radial projections perpendicular to the

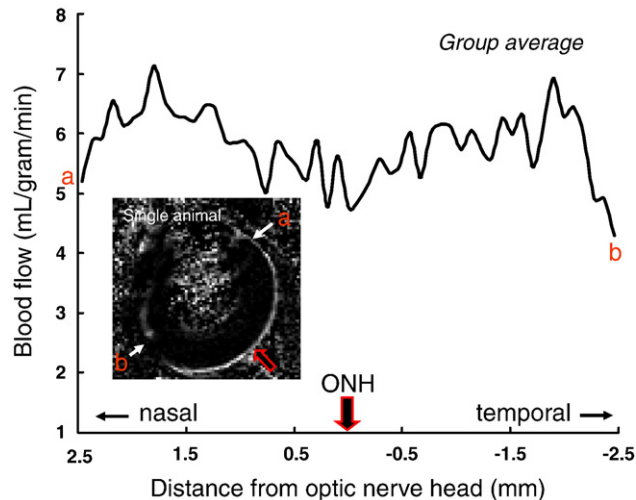


Fig. 3. Blood-flow values as a function of distance from the optic nerve head (ONH). Data were obtained from one distal edge to another (points a to b). Blood-flow values were taken at the peaks of the projection profiles.

vitreous boundary were then obtained with (3×) spatial interpolation. Some interpolations were necessary for the profile analysis to be completely automated and such spatial interpolation was previously confirmed not to significantly alter peak width and height (Cheng et al., 2006). Blood-flow values for the entire retinal thickness were determined as a function of distance from the optic nerve head. Blood-flow profiles were also plotted across the thickness of the retina and averaged along the entire length of the retina. Blood-flow values were taken at the peaks of the profiles.

Results

A cartoon of a rat eye, depicting the retina, cornea, vitreous, ciliary body, and sclera is shown in Fig. 1. Phantom and *in vivo* experiments showed that drift and motion artifacts across time series were <1 pixel in the retina, indicative of stability of blood-flow measurements (see Discussion for details).

Quantitative basal blood-flow images (Fig. 2) showed that blood-flow values in the retina and the ciliary body were the

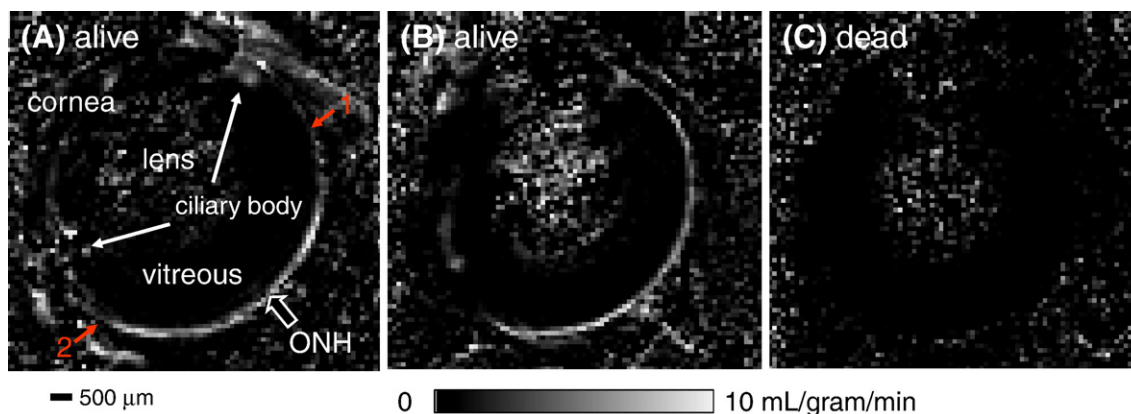


Fig. 2. Cross-sectional images showing quantitative basal blood-flow images. Blood-flow images were obtained from (A, B) alive and (C) dead animal (B and C from the same animal). Blood-flow values in the retina and the ciliary body are high, whereas blood flow in the lens and vitreous was within noise levels. The big arrows indicate the locations of the optic nerve head (ONH). Blood-flow values in Table 1 and Fig. 5 were averaged from points 1 to 2, ignoring the distal edges of the retina.

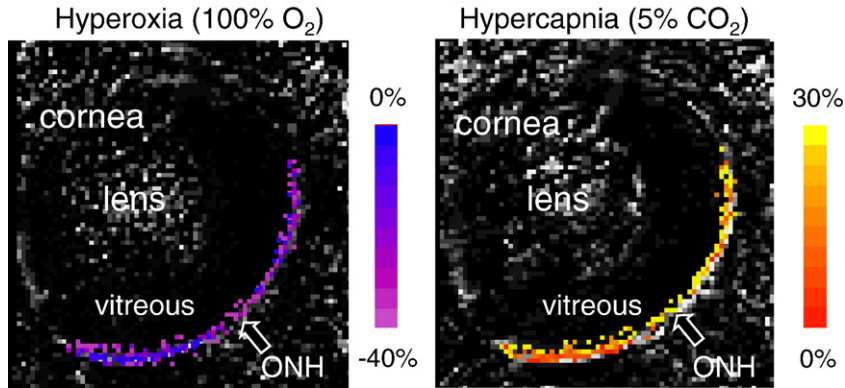


Fig. 4. Blood-flow percent-change maps responding to physiologic stimuli (100% O₂ or 5% CO₂) obtained from one representative animal. Percent-change color maps are overlaid on blood-flow images. Color bars indicate blood-flow percent changes. ONH: optic nerve head.

highest, whereas blood flow in the lens, cornea, and vitreous were within noise level. Blood flow was confirmed as the source of the signals by repeating measurements after rats were sacrificed in the scanner. Blood-flow images of the post-mortem animals revealed no statistically significant blood-flow contrast in the retina (Fig. 2C, average: 0.03 ± 0.01 ml/g/min, N=3). Fig. 3 shows the group-average blood flow as a function of distance from the optic nerve head. Blood flow is relatively constant across the length of the retina, except it dipped slightly at the optic nerve head and dropped significantly at the distal edges where the retina terminates.

Physiological stimuli evoked robust blood-flow changes in the retina. Fig. 4 shows the blood-flow percent-change maps associated with hyperoxia and hypercapnia from one representative animal. Hyperoxia decreased blood flow, whereas hypercapnia increased blood flow. To avoid bias of using region-of-interest analysis, blood-flow profiles across the thickness of the retina (from sclera to vitreous) before and during physiologic challenges were analyzed (Fig. 5). Blood flow in the retina was markedly above noise level as indicated by the negligible blood-flow values in the vitreous and sclera on either side of the peak. The group-average full-width at half maximum (FWHM) of the blood-flow

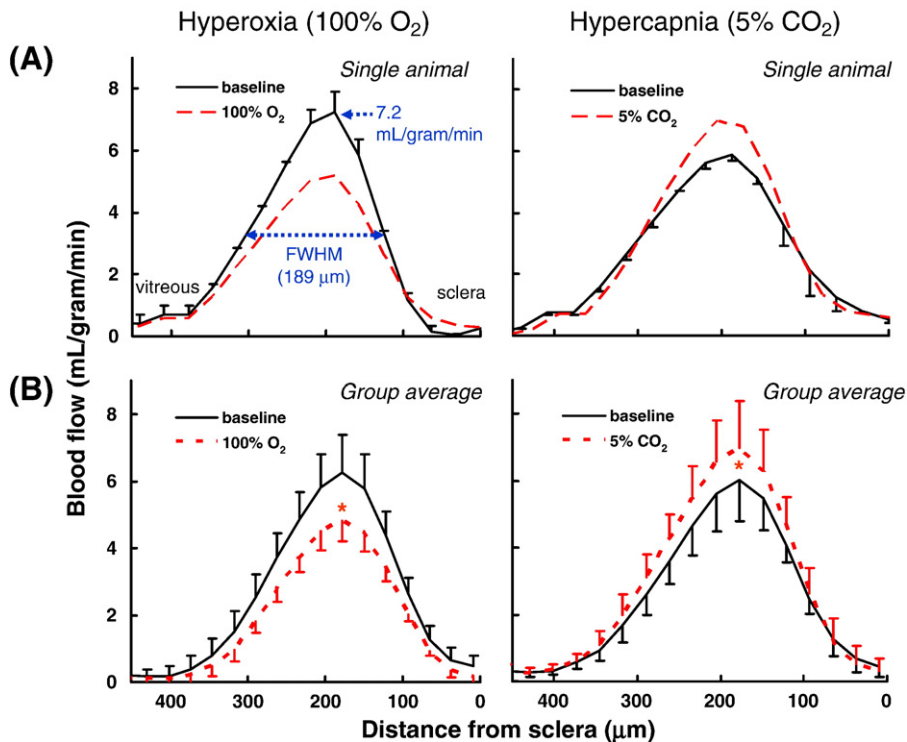


Fig. 5. Blood-flow projection profiles across the retinal thickness under baseline, 5% CO₂, and 100% O₂ challenges from (A) a single animal and (B) group-average data. The full-width at half maximum (FWHM) of the blood-flow profile was 200 μm (group-average value: 181 ± 23 μm). The error bars in panel A are those of three repeated measurements from one animal (group-average intra-subject variation=8.7%). The error bars in panel B are inter-subject variations. Blood-flow changes due to hyperoxia and hypercapnia were statistically significantly different from baseline (air) (* indicates $P < 0.05$).

Table 1

Blood flow (ml/g/min) of the retina before and during physiologic challenges under 1.0% isoflurane, and basal blood flow under 1.5% isoflurane

Air (1.0% isoflurane) N=6	100% O ₂ N=6	5% CO ₂ N=6	Air (1.5% isoflurane) N=4
6.3±1.0	4.8±0.6 ^a	7.3±1.1 ^b	9.3±2.7 ^c
N/A	(−25±6%)	(16±6%)	(48%)

Data under 1.5% isoflurane were obtained from a separate group of animals. Blood-flow values were taken at the peaks of the projection profiles. Relative to baseline (air), a: $P=0.0004$ (paired t -test), b: $P=0.002$ (paired t -test), and c: $P=0.006$ (unpaired t -test).

profile was 181 ± 23 μm . This is not the same as the anatomical thickness of the retina (267 ± 31 μm , including the *choroid*) reported previously (Cheng et al., 2006). Group-averaged basal blood flow and blood-flow changes due to hyperoxia and hypercapnia are summarized in Table 1.

To further demonstrate the sensitivity of the technique, blood-flow measurements were also made at two different isoflurane concentrations in air. Blood flow increased from 6.3 ± 1.0 ml/g/min under 1.0% isoflurane to 9.3 ± 2.7 ml/g/min under 1.5% isoflurane ($P=0.006$) (Table 1).

Discussion

This study reports a proof-of-concept that quantitative basal blood flow, and physiologically induced and isoflurane-induced blood-flow changes in the retina can be imaged using the arterial spin-labeling technique. The unique advantages of MRI blood-flow measurements are: (1) non-invasive, (2) without depth limitation, and (3) quantitative which allows comparison across animals. MRI thus has the potential to provide a valuable tool to study how blood flow is regulated in the retina and how retinal diseases may affect blood flow and the tissue they subserve.

Potential issues

Proper interpretation of MRI blood-flow data requires careful consideration of three major potential issues, namely, drift and movement artifact, assumptions in blood-flow calculation, and partial-volume effects.

Potential drift and movement artifact

High-resolution blood-flow imaging of the retina is more susceptible to potential drift and movement artifacts because: (i) High-resolution imaging pulse sequence is more demanding on the magnetic field gradient, which could lead to temperature-induced frequency and signal drift. The exact sources of this temperature-dependent drift could come from the gradient *per se*, cryostat and/or passive shims. (ii) The relatively small pixel size compared to conventional brain MRI could be more sensitive to drift. (iii) The thin retina is bounded by the sclera and the vitreous which have very different signal intensities than the retina. Mis-registration of the time-series images could thus lead to significant errors. (iv) Finally, ASL blood-flow MRI requires subtraction of paired images and is thus more susceptible to motion that may occur between acquisitions of the paired images.

To address these potential issues, phantom studies were performed to distinguish potential hardware-related from animal-

related instability. The second-order Z2 shims which generally have a long time constant to reach steady state were observed to cause majority of the temperature-induced drift in the MRI signals on phantoms. The solution was either to leave the high-order shim currents on at the typical values overnight or avoid using second-order shims (third-order shims were not explored). Consequently, hardware-related instability was essentially eliminated. In regard to animal preparation, the combination of isoflurane anesthetic and pancuronium paralytic has been previously demonstrated to yield stable animal preparation over similarly long imaging time (Cheng et al., 2006).

To ensure *in vivo* MRI data were free of significant movement and drift artifacts, the following evaluations were performed. All images were acquired in time series and co-registered if needed before additional data processing (i.e., signal averaging and cross-correlation analysis). Time-loop movies and center-of-mass time courses were evaluated. Signal time courses were also evaluated to ensure no sudden jump or significant drift. These evaluations provided sensitive indicators because signal contamination from either side of the retina due to mis-registration would markedly affect signal intensities.

Quantitative blood-flow calculation

Quantitative blood-flow measurements are generally difficult and all quantitative blood-flow techniques, including the commonly used MRI, positron emission tomography, hydrogen clearance, and microsphere techniques, have their own strengths and limitations. The continuous ASL technique applied herein has the following limitations. Blood-flow calculation used the blood-tissue partition coefficient (λ) of the brain (Herscovitch and Raichle, 1985) because blood-tissue partition coefficient in the retina has not been measured. This is, however, justified because the retina is part of the central nervous system. In addition, brain T_1 was used in the blood-flow calculation. Preliminary measurements showed that retina T_1 is similar to brain T_1 (unpublished data). T_2 and apparent diffusion coefficient the retina have been reported to be similar to those of the brain (Shen et al., 2006). Labeling duration was 2.9 s which is significantly longer than tissue T_1 and thus the *continuous* ASL condition was satisfied. The effect of transit time in the rat retina was justly ignored because the transit time is sufficiently short (ca. ~ 200 ms) compared to blood T_1 , as it is the case for calculating cerebral blood flow in rats. While there is no gold standard to validate quantitative blood flow obtained with MRI, blood-flow MRI has been cross-validated with PET and autoradiographic techniques in the brain. Improving accuracy of quantitative blood-flow MRI remains an active area of research.

Partial-volume effect (PVE)

While the MRI spatial resolution is high compared to those typically employed for rat brain imaging, PVE due to the thin retina could potentially be significant. Given the thin retina of 267 μm (Cheng et al., 2006), the in-plane resolution of 90×90 μm yielded ~ 3 pixels across the retinal thickness. This resolution prevented reliable analysis of blood flow in different layers within the retina. Future studies will need to improve spatial resolution and sensitivity to differentiate blood flow between the *retinal* and *choroidal* vasculature. Nonetheless, the current spatial resolution is sufficient to robustly measure total blood flow and blood-flow changes across the entire retinal thickness.

Imaging quantitative blood flow

Blood flow in the retina and the ciliary body was high whereas blood flow in the cornea and vitreous was essentially absent or within noise level. These results are consistent with those reported using microsphere technique (Alm and Bill, 1973). Blood-flow signals in the lens and the ocular muscle appeared “noisier” than those in the vitreous and the retina in both live and post-mortem animals (Fig. 2). This is because of the short T_2^* in the lens, and the relatively low blood flow in the ocular muscle which results in poorer signal-to-noise ratio of the EPI, leading to “division” errors in the blood-flow calculation. Nonetheless, these “noisy” pixels averaged to zero post-mortem.

Basal blood flow of the retina, including the choroid, under 1% isoflurane (6.3 ± 1.0 ml/g/min) is markedly higher than cerebral blood flow, which have been reported to be 0.9 ± 0.13 ml/g/min (Liu et al., 2004) and 1.1 ± 0.04 ml/g/min (Sicard and Duong, 2005) under essentially identical experimental conditions. The blood-flow values reported at current spatial resolution are a weighted average of the *retinal* and *choroidal* blood flow. *Retinal* blood flow is similar to cerebral blood flow in the gray matter whereas *choroidal* blood flow is about 10 times higher than cerebral blood flow using microsphere technique in monkeys (Alm and Bill, 1973). Another microsphere study in rats also reported that *choroidal* blood flow is 9.5 times higher than *retinal* blood flow (Wang et al., 2007). Microsphere techniques typically report blood flow in units of ml/min and thus direct quantitative comparison is difficult. The overall blood flow in the retina herein is heavily weighted by that of the *choroid*. High *choroidal* blood flow appears to be in excess of local metabolic requirements, and may be necessary to maintain a large oxygenation gradient (Linsenmeier and Padnick-Silver, 2000) and to dissipate heat produced by light (Parver, 1980; Parver et al., 1982).

Blood flow showed a weak spatial dependence as a function of distance from the optic nerve head (note that rat does not have a fovea). Blood flow dipped slightly at the optic nerve head relative to its immediate surrounding. This may appear to contradict the notion that the optic nerve head is densely populated by large arteries and veins. However, the ASL technique is mostly sensitive to smaller vessels (such as arterioles, capillaries and venules) because the short transit time in rat allows the bolus of magnetically tagged water spins to exit large arteries when image acquisition occurs and most of the T_1 -based blood-flow contrast is attenuated when blood reaches large draining veins (Duong et al., 2001; Calamante et al., 2002). Thus, it is not surprising that blood flow in the optic nerve head measured by the ASL technique is similar to, or even lower than, its surrounding tissue. Moreover, stimulus-evoked blood-flow changes are expected to be negligible in large veins and arteries compared to smaller vessels because these large vessels are known not to significantly vasoreact to blood-flow modulators such as CO_2 and stimuli to increase neural activity. Improved blood-flow sensitivity to smaller vessels is advantageous because blood flow in smaller vessels reflects more accurately local tissue perfusion.

Blood flow was observed to drop significantly at the distal edges of the retina, consistent with those reported previously (Alm and Bill, 1973). This is expected because the retina terminates at the distal edges where it has less metabolic and blood-flow demands compared to the central part of the retina. To our knowledge, this is the first *in vivo* blood-flow measurement along the entire length of the retina *in vivo*, in contrast to the optically

based imaging techniques which have limited field of view constrained by illumination angle.

Imaging vascular reactivity

Neurovascular coupling of blood flow, metabolism, and function in the brain has been well described. Experimental evidence of such coupling in the retina has only been reported recently. For example, flickering light increases blood flow in optic nerve head as detected by LDF (Riva et al., 1991). Physiologic stimuli with oxygen or carbogen modulate tissue oxygenation as measured by oxygen polarographic electrodes (Yu et al., 2000). Visual stimulation modulates optical absorption as detected by intrinsic optical imaging (Nelson et al., 2005; Tso et al., 2006). Physiologically evoked changes in blood flow were recently reported by laser speckle imaging with large FOV (Cheng and Duong, 2007). Physiologically evoked (Cheng et al., 2006) and visually evoked (Duong et al., 2002) changes of blood oxygenation in the retina can be detected by BOLD functional MRI.

Hyperoxia

Oxygen inhalation causes vasoconstriction, resulting in blood-flow reduction of $25 \pm 6\%$. Given our spatial resolution, the blood-flow percent change is a weighted average of the changes in the *retinal* and *choroidal* vasculatures. Oxygen breathing has been reported to decrease *retinal* blood flow by 30% using Heidelberg Retina Flowmeter (Stern et al., 1997), 36% using blue-field entoptic technique (Fallon et al., 1985), and 60% using LDF (Trokel, 1965; Eperon et al., 1975; Riva et al., 1983). In contrast, inhalation of oxygen has little or no effect on *choroidal* blood flow in the macular region (Riva et al., 1994; Schmetterer et al., 1995; Schmetterer et al., 1996). Taken together, the measured blood-flow changes by MRI are nonetheless sensitive to changes in *retinal* vasculature, although basal blood flow is weighted heavily by the high basal blood flow in the *choroid* which does not vasoreact to hyperoxia.

In the brain, oxygen inhalation in awake humans elicits only 13% cerebral blood-flow reduction (Kety and Schmidt, 1948). Given that the blood-flow change is a weighted average of the *retinal* and *choroidal* vasculatures and the *choroid* does not significantly respond to hyperoxia, hyperoxia-induced vasoconstriction in the *retinal* vessels appears to be significantly stronger than that in the brain vessels.

Hypercapnia

Hypercapnic (5% CO_2 in air) inhalation causes vasodilation, resulting in a blood-flow increase of $16 \pm 6\%$. While there are some evidence that hypercapnia elicits vasodilation in both *retinal* and *choroid* blood vessels using LDF and microsphere techniques (Alm and Bill, 1972a,b; Friedman and Chandra, 1972; Cioffi et al., 2003), their literatures are sparse and inconsistent. Inhalation of 10% CO_2 in air showed no significant vasodilation in the *retinal* vessels (Frayser and Hickam, 1964). Inhalation of carbogen (95% $\text{O}_2 + 5\% \text{CO}_2$) increased *choroid* blood flow by $12.5 \pm 11.7\%$ with large inter-subject variations (Geiser et al., 2000). At higher CO_2 concentrations, however, *retinal* blood flow was observed to increase 240% and *choroidal* blood flow was observed to increase 150% (arterial $\text{pCO}_2 = 80.9$ mm Hg, which we estimated to be $>15\% \text{CO}_2$) (Alm and Bill, 1972a). Our results indicate that there is consistent and significant blood-flow increase with 5% CO_2 inhalation in the overall retina. These discrepancies could be due to

differences in techniques and their signal sources and require further investigation.

In the rat brain, hypercapnic (5% CO₂ in air) inhalation increased cerebral blood flow by 25% (Sicard et al., 2003b) and 52% (Sicard and Duong, 2005) in rats under essentially identical experimental conditions (except the animals breathed spontaneously). The difference between spontaneous breathing in this study could not explain the difference in response magnitude because animals under spontaneous breathing increase respiration rate which should slightly reduce blood CO₂ (Sicard and Duong, 2005). Similar hypercapnia-induced changes in cerebral blood flow in awake humans and animals under different anesthetics have also been reported in the literatures, although quantitative comparison is less informative due to differences in experimental conditions. In short, hypercapnia-induced blood-flow increase appears to be smaller in the retina than in the brain. This may be due to the high basal *choroidal* blood flow, which could reduce head room for additional vasodilation (Sicard and Duong, 2005). The use of isoflurane could further accentuate this effect.

Effects of vasodilator on blood flow in the retina

Isoflurane was observed to have profound effects on blood flow in the retina. Blood flow in the retina under 1.0% isoflurane was 6.3 ± 1.0 ml/g/min and it increased to 9.3 ± 2.7 ml/g/min under 1.5% isoflurane (48% increase). This is consistent with the notion that isoflurane is a known vasodilator (Matta et al., 1999) which has been well documented in the brain. In fact, cerebral blood flow under ~1% isoflurane (1.27 ± 0.29 ml/g/min) is higher than awake restrained conditions (0.86 ± 0.25 ml/g/min) in the same animals (Sicard et al., 2003a). Increasing isoflurane concentration from 1% to 2% increases cerebral blood flow from 0.87 ± 0.27 to 1.31 ± 0.30 ml/g/min in the same animals (Duong and Kim, 2000). Isoflurane appears to have overall similar vasodilatory effects on vessels in the retina as in the brain, although differential effects on *retinal* and *choroidal* vessels may exist and remain to be investigated.

Finally, we would like to reiterate that caution must be exercised when comparing blood-flow measurements among LDF, microsphere, and MRI techniques because they have different signal sources. Microsphere techniques may be susceptible to post-mortem artifacts and the reported blood-flow values may vary depending on microsphere size and concentration (Kuznetsova et al., 1998). LDF measures a single point and is likely more sensitive to large vessels. *Retinal* blood flow measured using LDF is contaminated by *choroidal* blood flow to some extent because of its lack of depth resolution, and *choroid* blood flow is limited to the macular region where *retinal* vessels are absent. Blood-flow MRI measures a larger area and is more sensitive to smaller vessels, but takes significantly longer to acquire and has lower spatial resolution compared to some optically based imaging techniques. At the current spatial resolution, the measured blood flow is a weighted average of *retinal* and *choroid* vasculature. Non-invasive blood-flow MRI has no depth limitation and, thus, has the unique potential to image layer-specific blood flow if higher spatial resolution can be achieved.

Conclusions

In summary, we demonstrate a proof of principle that quantitative basal blood flow in the thin retina and its responses

to physiologic stimuli can be reliably imaged using non-invasive, high-resolution MRI without depth limitation. Future studies will focus on improving spatial resolution to distinguish lamina-specific blood flow in the *retinal* and *choroidal* vasculature, and to investigate visually evoked blood-flow responses. MRI has the potential to provide unique information on how blood flow is regulated and how retinal diseases may affect blood flow and the neural tissues they subserve. While the non-invasive nature of MRI could streamline human applications, much work remains to be done before clinical applications can be contemplated. Nonetheless, this technique should readily provide a valuable tool to study retinal diseases in animal models.

Acknowledgments

The authors thank Dr. Qiang Shen, PhD, for help with the ASL technique. This work was supported by the NIH/NEI (R01EY014211), VISN7 Career Development Award from the Department of Veterans Affairs, and the Ophthalmology Core grant (P30 EY006360). The Yerkes Imaging Center is supported in part by the NCRR (P51 RR00165).

References

- Alm, A., Bill, A., 1972a. The oxygen supply to the retina: II. Effects of high intraocular pressure and of increased arterial carbon dioxide tension on uveal and retinal blood flow in cats. *Acta Physiol. Scand.* 84, 306–319.
- Alm, A., Bill, A., 1972b. The oxygen supply to the retina: I. Effects of changes in intraocular and arterial blood pressures, and in arterial pO₂ and pCO₂ on the oxygen tension in the vitreous body of the cat. *Acta Physiol. Scand.* 84, 261–274.
- Alm, A., Bill, A., 1973. Ocular and optic nerve blood flow at normal and increased intraocular pressures in monkeys (*Macaca irus*): a study with radioactively labelled microspheres including flow determinations in brain and some other tissues. *Exp. Eye Res.* 15, 15–29.
- Barbier, E.L., Liu, L., Grillon, E., Payen, J.F., Lebas, J.F., Segebarth, C., Remy, C., 2005. Focal brain ischemia in rat: acute changes in brain tissue T1 reflect acute increase in brain tissue water content. *NMR Biomed.* 18, 499–506.
- Berkowitz, B.A., Roberts, R., Goebel, D.J., Luan, H., 2006. Noninvasive and simultaneous imaging of layer-specific retinal functional adaptation by manganese-enhanced MRI. *Invest. Ophthalmol. Visual Sci.* 47, 2668–2674.
- Calamante, F., Gadian, D.G., Connelly, A., 2002. Quantification of perfusion using bolus tracking magnetic resonance imaging in stroke: assumptions, limitations, and potential implications for clinical use. *Stroke* 33, 1146–1151.
- Cheng, H., Duong, T.Q., 2007. Simplified laser-speckle-imaging analysis method and its application to retinal blood flow imaging. *Opt. Lett.* 32, 2188–2190.
- Cheng, H., Nair, G., Walker, T.A., Kim, M.K., Pardue, M.T., Thule, P.M., Olson, D.E., Duong, T.Q., 2006. Structural and functional MRI reveals multiple retinal layers. *Proc. Natl. Acad. Sci. U. S. A.* 103, 17525–17530.
- Cioffi, G.A., Granstam, E., Alm, A., 2003. Adler's physiology of the eye. In: Kaufman, P.L., Alm, A. (Eds.), *Clinical Application*. Mosby, St. Louis, pp. 747–784.
- Duong, T.Q., Kim, S.-G., 2000. In vivo MR measurements of regional arterial and venous blood volume fractions in intact rat brain. *Magn. Reson. Med.* 43, 392–402.
- Duong, T.Q., Kim, D.-S., Ugurbil, K., Kim, S.-G., 2001. Localized blood flow response at sub-millimeter columnar resolution. *Proc. Natl. Acad. Sci. U. S. A.* 98, 10904–10909.

- Duong, T.Q., Ngan, S.-C., Ugurbil, K., Kim, S.-G., 2002. Functional magnetic resonance imaging of the retina. *Invest. Ophthalmol. Visual Sci.* 43, 1176–1181.
- Eperon, G., Johnson, M., David, N.J., 1975. The effect of arterial PO₂ on relative retinal blood flow in monkeys. *Invest. Ophthalmol. Visual Sci.* 14, 342–352.
- Fallon, T.J., Maxwell, D.L., Kohner, E.M., 1985. Retinal vascular autoregulation in conditions of hyperoxia and hypoxia using the blue field entopic phenomenon. *Ophthalmology* 92, 701–705.
- Formaz, F., Riva, C.E., Geiser, M., 1997. Diffuse luminance flicker increases retinal vessel diameter in human. *Curr. Eye Res.* 16, 1252–1257.
- Frayser, R., Hickam, J.B., 1964. Retinal vascular response to breathing increased carbon dioxide and oxygen concentrations. *Invest. Ophthalmol. Visual Sci.* 3, 427–431.
- Friedman, E., Chandra, S.R., 1972. Choroidal blood flow: III. Effects of oxygen and carbon dioxide. *Arch. Ophthalmol.* 87, 70–71.
- Geiser, M.H., Riva, C.E., GDorner, G.T., Diermann, U., Luksch, A., Schmetterer, L., 2000. Response of choroidal blood flow in the foveal region to peroxia and hyperoxia-hypercapnia. *Curr. Eye Res.* 21, 669–676.
- Guyer, D.R., Yannuzzi, L.A., Slakter, J.S., Sorenson, J.A., Orlock, S., 1993. The status of indocyanine-green videoangiography. *Curr. Opin. Ophthalmol.* 4, 3–6.
- Harris, A., Kagemann, L., Cioffi, G.A., 1998. Assessment of human ocular hemodynamics. *Surv. Ophthalmol.* 42, 509–533.
- Herscovitch, P., Raichle, M.E., 1985. What is the correct value for the brain–blood partition coefficient for water? *J. Cereb. Blood Flow Metab.* 5, 65–69.
- Kety, S.S., Schmidt, C.F., 1948. The effects of altered arterial tensions of carbon dioxide and oxygen on cerebral blood flow and cerebral oxygen consumption of normal young men. *J. Clin. Invest.* 27, 484–491.
- Kuznetsova, L.V., Tomasek, N., Sigurdsson, G.H., Banic, A., Erni, D., Wheatley, A.M., 1998. Dissociation between volume blood flow and laser-Doppler signal from rat muscle during changes in vascular tone. *Am. J. Physiol.* 274, H1248–H1254.
- Linsenmeier, R.A., Padnick-Silver, L., 2000. Metabolic dependence of photoreceptors on the choroid in the normal and detached retina. *Invest. Ophthalmol. Visual Sci.* 41, 3117–3123.
- Liu, Z.M., Schmidt, K.F., Sicard, K.M., Duong, T.Q., 2004. Imaging oxygen consumption in forepaw somatosensory stimulation in rats under isoflurane anesthesia. *Magn. Reson. Med.* 52, 277–285.
- Matta, B.F., Heath, K.J., Tipping, K., Summors, A.C., 1999. Direct cerebral vasodilatory effects of sevoflurane and isoflurane. *Anesthesiology* 91, 677–680.
- Nelson, D.A., Krupsky, S., Pollack, A., Aloni, E., Belkin, M., Vanzetta, I., Rosner, M., Grinvald, A., 2005. Special report: noninvasive multiparameter functional optical imaging of the eye. *Ophthalmic Surg. Lasers Imaging* 36, 57–66.
- Parver, L.M., 1980. Choroidal blood flow as a heat dissipating mechanism in the macula. *Am. J. Ophthalmol.* 89, 641–646.
- Parver, L.M., Auker, C.R., Carpenter, D.O., Doyle, T., 1982. Choroidal blood flow. *Arch. Ophthalmol.* 100, 1327–1330.
- Preussner, P.R., Richard, G., Darrelmann, O., Weber, J., Kreissig, I., 1983. Quantitative measurement of retinal blood flow in human beings by application of digital image-processing methods to television fluorescein angiograms. *Graefes Arch. Clin. Exp. Ophthalmol.* 221, 110–112.
- Riva, C.E., Grunwald, J.E., Singclair, S.H., 1983. Laser Doppler velocimetry study of the effect of pure oxygen breathing on retinal blood flow. *Invest. Ophthalmol. Visual Sci.* 24, 47–51.
- Riva, C.E., Harino, S., Shonat, R.D., Petrig, B.L., 1991. Flicker evoked increase in optic nerve head blood flow in anesthetized cats. *Neurosci. Lett.* 128, 291–296.
- Riva, C.E., Cranstoun, S.D., Grunwald, J.E., Petrig, B.L., 1994. Choroidal blood flow in the foveal region of the human ocular fundus. *Invest. Ophthalmol. Visual Sci.* 35, 4273–4281.
- Riva, C.E., Logean, E., Falsini, B., 2005. Visually evoked hemodynamical response and assessment of neurovascular coupling in the optic nerve and retina. *Prog. Retin. Eye Res.* 24, 183–215.
- Schmetterer, L., Wolzt, M., Lexer, F., 1995. The effect of hyperoxia and hypercapnia on fundus pulsations in the macular and optic disc region in healthy young men. *Exp. Eye Res.* 61, 685–690.
- Schmetterer, L., Lexer, F., Findl, O., Grasse, U., Eichler, H.G., Wolzt, M., 1996. The effect of inhalation of different mixtures of O₂ and CO₂ on ocular fundus pulsation. *Exp. Eye Res.* 63, 351–355.
- Shen, Q., Ren, H., Cheng, H., Fisher, M., Duong, T.Q., 2005. Functional, perfusion and diffusion MRI of acute focal ischemic brain injury. *J. Cereb. Blood Flow Metab.* 25, 1265–1279.
- Shen, Q., Cheng, H., Chang, T.F., Nair, G., Shonat, R.D., Pardue, M.T., Toi, V.V., Duong, T.Q., 2006. Magnetic resonance imaging of anatomical and vascular layers of the cat retina. *J. Magn. Reson. Imaging* 23, 465–472.
- Sicard, K.M., Duong, T.Q., 2005. Effects of hypoxia, hyperoxia and hypercapnia on baseline and stimulus-evoked BOLD, CBF and CMRO₂ in spontaneously breathing animals. *NeuroImage* 25, 850–858.
- Sicard, K., Shen, Q., Brevard, M., Sullivan, R., Ferris, C.F., King, J.A., Duong, T.Q., 2003a. Regional cerebral blood flow and BOLD response in conscious and anesthetized rats under basal and hypercapnic conditions: implications for fMRI studies. *J. Cereb. Blood Flow Metab.* 23, 472–481.
- Sicard, K., Shen, Q., Brevard, M.E., Sullivan, R., Ferris, C.F., King, J.A., Duong, T.Q., 2003b. Regional cerebral blood flow and BOLD responses in conscious and anesthetized rats under basal and hypercapnic conditions: implications for functional MRI studies. *J. Cereb. Blood Flow Metab.* 23, 472–481.
- Sternn, K., Manapace, R., Rainer, G., Findl, O., Wolzt, M., Schmetterer, L., 1997. Reproducibility and sensitivity of scanning laser Doppler flowmetry using graded changes in PO₂. *Br. J. Ophthalmol.* 81, 360–364.
- Trokel, S., 1965. Effect of respiratory gases upon choroidal hemodynamics. *Arch. Ophthalmol.* 73, 838–842.
- Tso, D.Y., Schallek, J., MZarella, M., Ghim, M., Abramoff, M., Kwon, Y., Kardon, R., Pokorny, J., Soliz, P., 2006. Pharmacological Dissection of Laminar Contributions to Intrinsic Optical Signals in the Retina. *Invest. Ophthalmol. Visual Sci.* 2006 47, E-Abstract 5899.
- Wang, L., Fortune, B., Cull, G., McElwain, K.M., Cioffi, G.A., 2007. Microspheres method for ocular blood flow measurement in rats: size and dose optimization. *Exp. Eye Res.* 84, 108–117.
- Williams, D.S., Detre, J.A., Leigh, J.S., Koretsky, A.P., 1992. Magnetic resonance imaging of perfusion using spin inversion of arterial water. *Proc. Natl. Acad. Sci. U. S. A.* 89, 212–216.
- Yu, D.-Y., Cringle, S.J., Su, E.-N., Yu, P.K., 2000. Intraretinal oxygen levels before and after photoreceptor loss in the RCS rat. *Invest. Ophthalmol. Visual Sci.* 41, 3999–4006.